

Coxibs interfere with the action of aspirin by binding tightly to one monomer of cyclooxygenase-1

Gilad Rimon^{a,b,1}, Ranjinder S. Sidhu^{a,1}, D. Adam Lauver^{c,1}, Jullia Y. Lee^a, Narayan P. Sharma^a, Chong Yuan^a, Ryan A. Frieler^a, Raymond C. Trievel^a, Benedict R. Lucchesi^c, and William L. Smith^{a,2}

^aDepartment of Biological Chemistry, University of Michigan, Ann Arbor, MI 48109; ^bDepartment of Clinical Pharmacology, Ben-Gurion University of the Negev, P.O. Box 653, Beer-Sheva 84105, Israel; and ^cDepartment of Pharmacology, University of Michigan, Ann Arbor, MI 48109

Communicated by Minor J. Coon, Victor C. Vaughan Distinguished University, Ann Arbor, MI, August 27, 2009 (received for review May 5, 2009)

Pain associated with inflammation involves prostaglandins synthesized from arachidonic acid (AA) through cyclooxygenase-2 (COX-2) pathways while thromboxane A₂ formed by platelets from AA via cyclooxygenase-1 (COX-1) mediates thrombosis. COX-1 and COX-2 are both targets of nonselective nonsteroidal antiinflammatory drugs (nsNSAIDs) including aspirin whereas COX-2 activity is preferentially blocked by COX-2 inhibitors called coxibs. COXs are homodimers composed of identical subunits, but we have shown that only one subunit is active at a time during catalysis; moreover, many nsNSAIDs bind to a single subunit of a COX dimer to inhibit the COX activity of the entire dimer. Here, we report the surprising observation that celecoxib and other coxibs bind tightly to a subunit of COX-1. Although celecoxib binding to one monomer of COX-1 does not affect the normal catalytic processing of AA by the second, partner subunit, celecoxib does interfere with the inhibition of COX-1 by aspirin in vitro. X-ray crystallographic results obtained with a celecoxib/COX-1 complex show how celecoxib can bind to one of the two available COX sites of the COX-1 dimer. Finally, we find that administration of celecoxib to dogs interferes with the ability of a low dose of aspirin to inhibit AA-induced ex vivo platelet aggregation. COX-2 inhibitors such as celecoxib are widely used for pain relief. Because coxibs exhibit cardiovascular side effects, they are often prescribed in combination with low-dose aspirin to prevent thrombosis. Our studies predict that the cardioprotective effect of low-dose aspirin on COX-1 may be blunted when taken with coxibs.

arachidonic acid | adrenic acid | nonsteroidal antiinflammatory drugs | platelet | prostaglandin

Prostaglandins (PGs) are oxygenated lipid mediators formed from the ω 6 essential fatty acid arachidonic acid (AA). The committed step in PG biosynthesis is the conversion of AA to PG H₂ (PGH₂) catalyzed by PG endoperoxide H synthase-1 or -2 commonly known as cyclooxygenase-1 and -2 (COX-1 and -2) (1–5). COX-1 and COX-2 are both targets of nonselective nonsteroidal antiinflammatory drugs (nsNSAIDs) including aspirin and ibuprofen, while COX-2 activity is selectively blocked by COX-2 inhibitors called coxibs (e.g., celecoxib) (6). Aspirin irreversibly acetylates Ser530 of COX-1 and COX-2 leading to enzyme inactivation (3). Because of its unusual pharmacokinetics, low doses of aspirin preferentially inhibit COX-1 in circulating platelets thereby attenuating platelet thromboxane synthesis and attendant thrombosis; thus, low-dose aspirin regimens are cardioprotective (6).

COX-1 and COX-2 are homodimers that exhibit half of sites enzymatic activity (7, 8), and many nsNSAIDs, apparently those involved in time-dependent inhibition, maximally inhibit the enzymes upon binding to only one monomer (7, 9). However, it appears that nsNSAIDs that are reversible, competitive inhibitors of COXs must bind to both monomers to cause enzyme inhibition (10). Similarly, fatty acids are bound to both monomers of a dimer during catalysis (8). Fatty acid binding to the first monomer transforms it to an allosteric monomer that, in turn,

modulates the substrate specificity of the second, now catalytically active, partner monomer.

Coxibs, at concentrations that do not inhibit COX-1 catalytic activity, have been reported to interfere with the abilities of nsNSAIDs including aspirin to inhibit COX-1 in vitro (11–14). This suggests that COX-2 inhibitors are able to bind to COX-1 and somehow compete with nsNSAID actions on COX-1 without affecting AA oxygenation. This is a potentially important clinical issue because many elderly patients take a combination of a coxib for pain relief and low-dose aspirin to counterbalance the potential cardiovascular side effects of coxibs (6, 15, 16).

Extensive clinical trial data on interactions between aspirin and coxibs are only available for one coxib, rofecoxib (16–19), and no significant effect on aspirin inhibition of thrombosis was detected. However, rofecoxib is the COX-2 inhibitor that is least effective in attenuating aspirin inhibition of COX-1 in vitro (14). Currently, the most widely used coxib is celecoxib. In two small trials with healthy human volunteers, the effects of aspirin were found not to be attenuated by celecoxib (15, 16); however, in both trials, the volunteers were given a 324 mg daily dose of aspirin, which is four times the dose of 81 mg commonly considered to be “low-dose” aspirin. In a potentially related study, celecoxib did attenuate aspirin inhibition in a dog model of thrombosis (20).

In the present study, we have used purified COX-1 to examine the interactions of celecoxib and other coxibs with aspirin and other nsNSAIDs in more detail. We find that celecoxib can bind to the COX active site of one monomer of COX-1 and interfere with the ability of aspirin to inhibit COX-1. We also find that the effect of low-dose aspirin on ex vivo platelet aggregation is blunted in dogs administered a combination of celecoxib and low-dose aspirin.

Results

Inhibition of COX-1 by Celecoxib and Other Coxibs. Inhibition of COX-2 by many nsNSAIDs and by coxibs including celecoxib has at least two phases. The first is a very rapid, second-order kinetic interaction, and this is followed by a much slower, first-order conformational rearrangement (9, 21–24). The intrinsic binding affinity of inhibitors for COXs can be estimated by measuring “instantaneous” inhibition that occurs when enzyme, substrate, and inhibitor are mixed without preincubating the

Author contributions: G.R., R.S.S., D.A.L., B.R.L., and W.L.S. designed research; G.R., R.S.S., D.A.L., J.Y.L., N.P.S., C.Y., and R.A.F. performed research; G.R., R.S.S., D.A.L., J.Y.L., C.Y., R.A.F., R.C.T., B.R.L., and W.L.S. analyzed data; W.L.S. wrote the paper.

The authors declare no conflict of interest.

Data deposition: The atomic coordinates have been deposited in the Protein Data Bank, www.rcsb.org (PDB ID code 3KK6).

¹G.R., R.S.S., and D.A.L. contributed equally to this study.

²To whom correspondence should be addressed at: Department of Biological Chemistry, University of Michigan Medical School, 1150 West Medical Center Drive, 5301 MSRB III, Ann Arbor, MI 48109-0606. E-mail: smithww@umich.edu.

This article contains supporting information online at www.pnas.org/cgi/content/full/0909765106/DCSupplemental.

inhibitor and enzyme (22). Consistent with previous studies (24), we found that celecoxib is more effective in causing instantaneous inhibition of COX-1 than COX-2 (IC_{50} values of 8.3 μ M vs. 15 μ M for COX-1 and COX-2, respectively) (Fig. S1). We also confirmed that, unlike the situation with COX-2, celecoxib is a freely reversible, competitive inhibitor of COX-1 (24). The fact that celecoxib is a freely reversible inhibitor of COX-1 suggests that celecoxib must bind to both monomers of COX-1 to cause enzyme inhibition (10). In contrast, time-dependent COX inhibitors studied to date function upon binding to one subunit of a COX dimer (7, 9). Thus, it is likely that COX-2 is inhibited when celecoxib binds to one monomer of COX-2. Consistent with this observation, we observed that, with AA as the substrate, celecoxib causes complete inhibition of COX-1, but a maximum of 80% inhibition of COX-2 (Fig. S1). We presume that, in the latter case, COX-2 celecoxib acts allosterically via one subunit of COX-2 to attenuate, but not completely inhibit, oxygenation in the partner catalytic subunit.

We also examined the ability of celecoxib to inhibit the oxygenation of adrenic acid (22:4 ω 6), a COX substrate homologous to AA for these studies (Fig. 1). Adrenic acid has very similar K_M values with COX-1 and COX-2 (8, 25). However, celecoxib was 15 times more potent in inhibiting adrenic acid oxygenation by ovine (ov) COX-1. Adrenic acid oxygenation by human (hu) COX-2 is not complete (55%) again because celecoxib acts allosterically via one subunit to attenuate, but not completely inhibit, oxygenation in the partner, catalytically functional subunit. Additionally, we observed that preincubation of celecoxib and COX-1 did not increase the level of inhibition of COX-1 when adrenic acid was used as the substrate (data not shown). This indicates that celecoxib is not a time-dependent inhibitor of adrenic acid oxygenation by COX-1. The results with AA vs. adrenic acid with celecoxib and COX-1 suggest that celecoxib competes more effectively with adrenic acid than AA for binding to the second monomer of COX-1. Taken together, the results imply that celecoxib must have a somewhat higher affinity for the allosteric monomer of COX-1 than the allosteric monomer of COX-2.

Coxibs Interfere with Inhibition of Purified COX-1 by Aspirin. Treatment of purified ovCOX-1 with radioactive aspirin (i.e., [14 C]-acetylsalicylate) led to a maximum incorporation of 0.96 ± 0.19 acetyl groups/dimer ($n = 9$) with COX-1, and inactivation was temporally correlated with acetylation (Fig. 2). Therefore, we conclude that aspirin acetylates only one monomer of a COX-1 dimer to cause complete loss of COX activity.

Previous studies have shown that low concentrations of coxibs that did not affect COX-1 activity attenuated the inhibition of COX-1 by aspirin in various cells and tissue extracts (11–14). Celecoxib is the most potent coxib in interfering with the effect

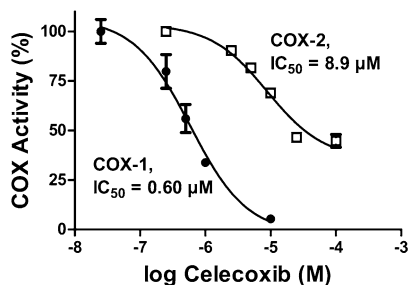


Fig. 1. Inhibition by celecoxib of the oxygenation of adrenic acid by ovCOX-1 and huCOX-2. Purified ovCOX-1 or huCOX-2 was added to assay samples containing 40 μ M adrenic acid and the indicated concentrations of celecoxib in an O_2 electrode assay chamber, and the rate of O_2 uptake was monitored to determine the level of instantaneous inhibition without the confounding, secondary effects of time-dependent inhibition (i.e., no preincubation of celecoxib with enzyme). Rates represent triplicate determinations \pm SE. The maximal level of inhibition achieved with celecoxib and huCOX-2 was the same when either 10 μ M or 40 μ M adrenic acid was used as substrate.

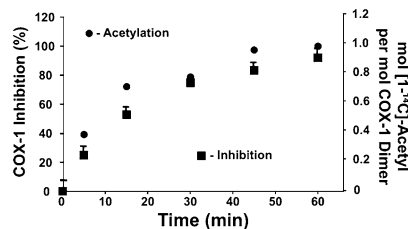


Fig. 2. Acetylation and inactivation of ovine cyclooxygenase-1 by aspirin. ovCOX-1 (7.6 μ M) was incubated at 37° with 1 mM [14 C-acetyl] aspirin for the indicated times and aliquots taken for measuring COX activity using a standard oxygen electrode assay and incorporation of the 14 C-acetyl group into protein. The percentage of acetylation was calculated based on the maximal level of acetylation by [14 C-acetyl] that was achieved following an overnight incubation.

of aspirin on COX-1 in human platelets (14), and so we focused on the effect of celecoxib on aspirin inhibition of COX-1. From the IC_{50} value for ovCOX-1 (Fig. S1), we calculated a K_i value of 1 μ M for instantaneous inhibition of AA oxygenation by celecoxib. We found that, under conditions in which celecoxib (2 or 4 μ M) would occupy less than 50% of available COX sites of the ovCOX-1 dimer (2 μ M of dimer), celecoxib attenuated the time-dependent inhibitory effect of aspirin on ovCOX-1 (Fig. 3A). Similarly, at concentrations of aspirin and celecoxib achieved in plasma with typical dosages of these drugs (26, 27), celecoxib largely prevented aspirin inhibition (Fig. 3B). The magnitude of the effect of celecoxib on aspirin action was similar to that observed with ibuprofen using a concentration of ibuprofen mimicking that achieved in human plasma and shown previously to attenuate aspirin inhibition *in vivo* (18, 28).

We next determined the effects of other coxibs including nimesulide, NS398, and DuP697 (6, 29, 30) on the sensitivity of purified ovCOX-1 to inhibition by aspirin and by two other nsNSAIDs—indomethacin (INDO) and ibuprofen. INDO is a time-dependent COX inhibitor, whereas ibuprofen is a freely reversible, competitive inhibitor (22). In a representative experiment (Fig. 4A), purified ovCOX-1 was preincubated in the presence or absence of DuP697 with or without INDO and then diluted into an assay chamber containing AA. DuP697 by itself, similar to NS398 (Fig. S2), had no effect on COX-1 activity with AA; however, when DuP697 was present, INDO caused 50% less inhibition than when DuP697 was absent. Similar results were obtained with INDO in combination with celecoxib, nimesulide, and NS398. The magnitude of the effects of the coxibs on COX-1 inhibition by INDO and aspirin were dependent on the coxib concentrations and the nsNSAID concentrations and the incubation times. In contrast to what was observed with the time-dependent nsNSAIDs, INDO, and aspirin, coxibs had no effect on the ability of the reversible nsNSAID ibuprofen to inhibit COX-1 activity with AA. This negative result is shown in Fig. 4B for the case of nimesulide in combination with ibuprofen.

Another key observation about the effects of coxibs on COX-1 is that, with NS398 and DuP697, the effects are only slowly reversible. For example, even when ovCOX-1 was washed extensively by buffer exchange following preincubation with NS398 or DuP697, the effects of these coxibs on COX-1 inhibition by INDO and aspirin remained. This is shown for the case of NS398 and INDO in Figs. S2 and S3. Similarly, when ovCOX-1 was preincubated with 25 μ M DuP697 for 30 min and then diluted 750-fold into an assay mixture containing AA (100 μ M) with or without an inhibitory concentration of INDO, the inhibition by INDO was still attenuated (Fig. S4). Thus, as seen with COX-2 (21, 23), NS398 and DuP697 appear to bind tightly to ovCOX-1 and dissociate slowly.

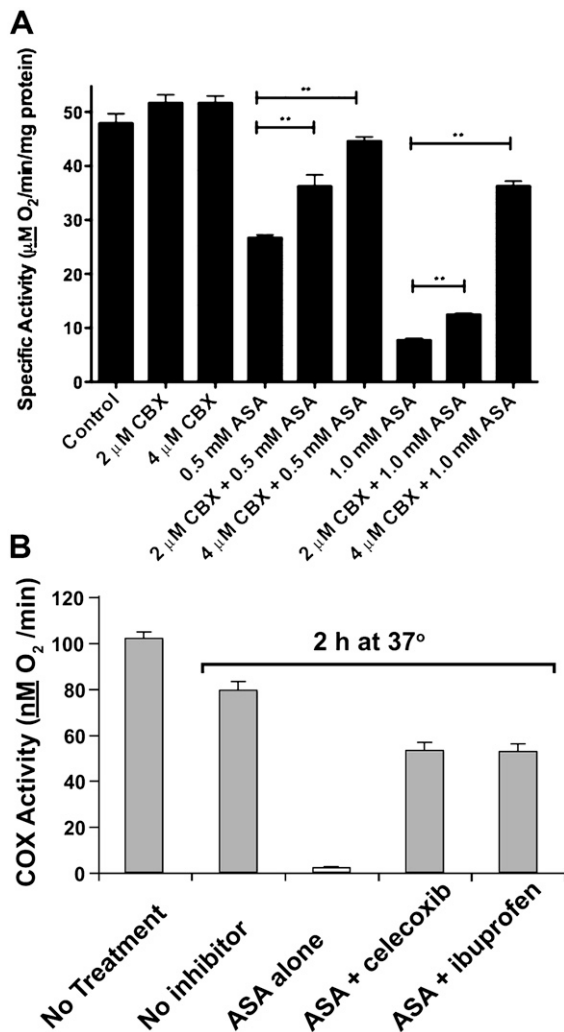


Fig. 3. Celecoxib attenuates the inhibition of ovCOX-1 by aspirin. (A) ovCOX-1 (2.0 μM) was preincubated with the indicated concentrations of aspirin and celecoxib at 37° for 1 h, and a small aliquot assayed for COX activity using an O_2 electrode with 40 μM AA as the substrate. When present, the concentrations of aspirin and celecoxib in the O_2 electrode assay chamber were 7.5 μM and 0.38 μM , respectively. Values are represented as mean \pm SEM, $n = 3$, and $**P < 0.0001$ vs. control using one-way ANOVA. (B) ovCOX-1 (2.0 μM) was not treated or was preincubated for 2 h at 37° with the indicated inhibitors (0.5 mM aspirin, 25 μM celecoxib, and 25 μM ibuprofen). Aliquots of the enzyme samples were assayed for COX activity as indicated above. Values are the average of triplicate determinations \pm SE.

Coxibs Bind to the COX Site of ovCOX-1. We employed x-ray crystallography to determine how celecoxib interacts with COX-1 (Fig. 5A–D, Table 1, Tables S1 and S2, and Figs. S5–S7). In the crystal of a celecoxib/ovCOX-1 complex, the pseudosymmetry ($P6_5/22$) could be partially deconvoluted in space group $P6_5$ using the mathematical twin operator ($h, -h, k, -l$) such that a structural bias is seen between partner monomers of the biological dimer. Electron density for celecoxib is present in the ovCOX-1 active site and nowhere else in the protein. The structure of the ovCOX-1 dimer suggests that the two monomers are different with one monomer (monomer A) fully occupied by celecoxib and the other monomer (monomer B) only partially occupied (*ca.* 50% estimated by group occupancy refinement and inhibitor/protein B-factor matching).

One notable difference in the active site of the celecoxib/ovCOX-1 complex compared with the reference model (ovCOX-1/ α -methyl-4-biphenylacetic acid complex 1Q4G) is in the

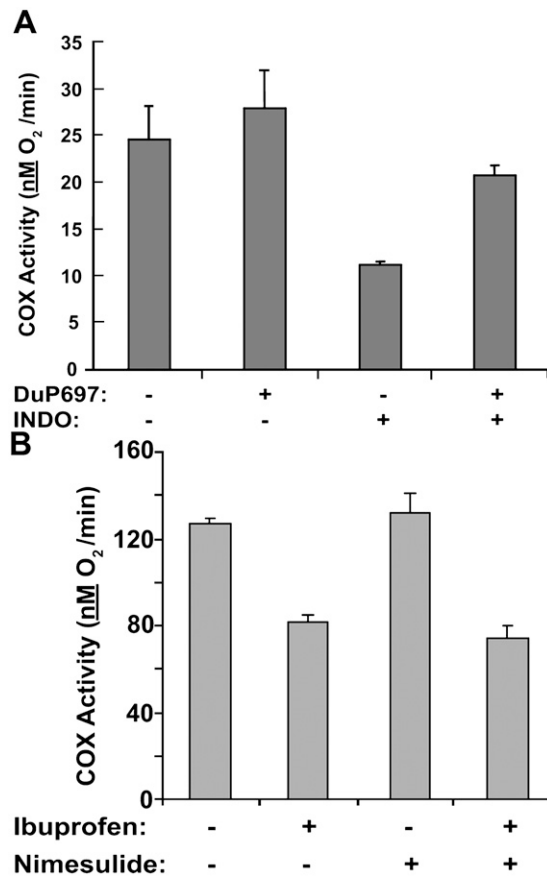


Fig. 4. Effects of coxibs on inhibition of ovCOX-1 by nsNSAIDs. (A) ovCOX-1 (0.70 μM) was preincubated with 10 μM DuP-697 and/or 10 μM indomethacin as indicated for 2 min at room temperature and a small aliquot assayed for COX activity using an O_2 electrode; when present, the final concentration of each inhibitor in the O_2 electrode assay chamber was 0.15 μM . Values are the average of triplicate determinations \pm SE. (B) ovCOX-1 was pretreated for 5 min at 37° with or without 10 μM nimesulide. Aliquots of the samples were then added to O_2 electrode assay chambers containing 20 μM AA and, as indicated, 10 μM nimesulide and/or 60 μM ibuprofen. Values are the average of triplicate determinations \pm SE. Similar results were obtained in testing the abilities of NS-398 and DuP-697 to interfere with the action of ibuprofen on ovCOX-1.

conformation of the terminal C δ 1 atom of Ile523 (Fig. 5A and B, and Fig. S5). This atom moves 3.1 Å compared to the same atom in the reference model to accommodate the benzene ring of celecoxib. It had been speculated that the size of Ile523, which is homologous to Val523 in COX-2, interfered with the binding of COX-2 inhibitors to COX-1 (31); however, a rotation in the dihedral angle $\text{C}\alpha\text{-C}\beta\text{-C}\gamma\text{1-C}\delta\text{1}$ from -69° (1Q4G) to 174° accommodates celecoxib binding. In addition, the Ile523 propagates a shift of side chain residues (His513, Pro514, and Asn515) in the β turn loop of the “side pocket” (residues 513–520) (Fig. 5B and Fig. S6). Curiously, the trifluoromethyl group on the pyrazole ring of celecoxib does not form contacts with Arg120 typically seen with substrates and carboxylic acid-containing inhibitors. Instead, the trifluoromethyl group abuts Tyr355 placing the phenol ring edge-to-face with the aromatic ring of the benzenesulfonamide group (Fig. 5B).

We compared the celecoxib/ovCOX-1 crystal structure with the structure of the related COX-2 selective inhibitor SC-558/murine (μ) COX-2 complex (32). A bromine atom in SC-558 substitutes for the methyl group in the distal aromatic ring of celecoxib. Both inhibitors bind in a similar manner with two exceptions. In μ -COX-2, Arg513, which is His513 in ovCOX-1, forms a hydrogen

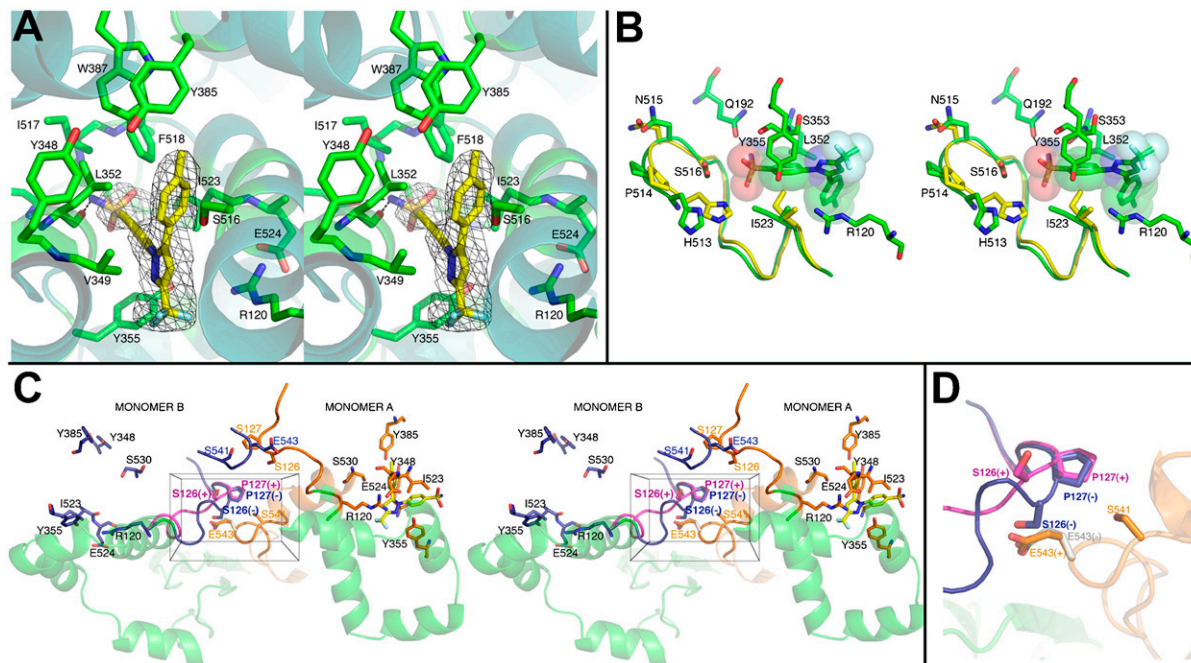


Fig. 5. Celecoxib binding to ovCOX-1 as determined by x-ray crystallography. (A) A stereoview of celecoxib (yellow) in the active site of COX-1 in the celecoxib/ovCOX-1 structure shown with omit $F_o - F_c$ difference density contoured at 2.8 σ (gray). Residues in the active site are displayed in green, whereas celecoxib is in yellow. Residues Arg120, Tyr355, and Glu524 lie at the mouth of the COX active site, whereas the catalytic Tyr385 hydrogen bonded to Tyr348 are located at the apex of the hydrophobic channel. (B) Stereoview of celecoxib/ovCOX-1 structure with the opening from the membrane binding domain into the COX active site oriented along plane of the page. Comparison of celecoxib/ovCOX-1 complex (green) and the reference model (1Q4G) (superimposed yellow ribbon and yellow side chains) shows that Ile523, homologous to Val523 in COX-2, adopts an extended rotamer conformation allowing access to the otherwise inaccessible hydrophobic side pocket comprised of residues Leu352, Ser353, Ile517, and Phe518 (some side chains are omitted for clarity). The residues His513 and Gln192 contribute to the outer shell of the side pocket and are included in the figure. Rendering of celecoxib atoms as spheres highlight the steric clash of Ile523 (yellow sticks in bottom panel) with the reference model. In Fig. S6 the positions of the α -carbons of residues 510–520 in the celecoxib/ovCOX-1 and the AA/ovCOX-1 (1DIY) structures relative to the reference model (1Q4G) are compared. (C) Stereoview of two alternate conformations of residues 121–129 in monomer B at the dimer interface traced into the electron density. Monomer A (orange) is shown with celecoxib bound (yellow) and monomer B is shown in the two conformations representing the conformation in the absence of bound inhibitor (blue) and the shift induced by binding of celecoxib (magenta). The side chains of Ser126 and Pro127 are shown in the two conformations and represented as inhibitor bound (+) and unbound (-) next to Glu543 (E543) of the partner monomer also in an alternate conformation. The position of celecoxib in monomer A (yellow sticks) and active site residues Arg120, Glu524, Tyr355, Ser530, and Tyr385 are shown for spatial orientation. Celecoxib in monomer B, which was refined to 50% occupancy in the final model, has been removed to represent the unbound monomer. (D) Enlarged view of the boxed area at the dimer interface shown in C.

bond with the sulfonamide group. In ovCOX-1, the more rigid histidine residue is more distant and does not form a hydrogen bond with celecoxib. We have placed the sulfonamide moiety of celecoxib such that the amide nitrogen makes short N-H-O hydrogen bonds with the side chain of Gln192 and main chain of Leu352 (Fig. S6). Additionally, the second shell residues of the side pocket Ile434 (Val434 in COX-2) are proposed to act as a gate to prevent Phe518 from moving away when bound to COX-2 selective inhibitors; however, in our structure, Phe518

side chain faces the inhibitor making hydrophobic contacts with the benzene ring in COX-1.

Refinement of the data using partial occupancy in monomer B showed clear positive $F_o - F_c$ difference density (i.e., unbiased electron density) in a loop involving residues 121–129 near the dimer interface (8, 32, 33) (Fig. 5C and D, Table 1, and Fig. S7). An alternate conformation of this loop in which residues 126 and 127 closely adjoin residues 543 and 541, respectively, on the partner monomer, was traced in monomer B (Fig. 5C and D, and Table 1). This alternate conformation is not visible in monomer A, which is fully occupied with celecoxib. We speculate that, in the absence of celecoxib, the loop involving residues 126 and 127 adopts a conformation not seen in other COX crystals, all of which have been prepared using a large excess of ligand over protein that fostered ligand binding to both monomers. Our crystallographic data are consistent with data obtained in examining oxidant-induced cross-linking of monomers of a cysteineless human COX-2 mutant in which new cysteines were engineered at positions 127 and 541 or 126 and 543 (8); binding of various nsNSAIDs and coxibs inhibited cross-linking between monomers of these mutant pairs. Additionally, the C β atoms of Ser126 and Glu543 are 3.7 Å apart within reasonable distance for disulfide bond formation.

Dogs Treated with Celecoxib Have an Attenuated Response to Low-Dose Aspirin. Ex vivo aggregation of platelets was measured using platelets isolated from blood drawn from dogs treated with

Table 1. Change in distance between C α main chain atoms of residues 121–129 located at the dimer interface in the bound vs. unbound conformations of the celecoxib/COX-1 complex

Amino acid	Distance between main chain C α , Å
121	1.08
122	1.57
123	5.93
124	3.42
125	5.23
126	1.91
127	0.22
128	0.25
129	0.39

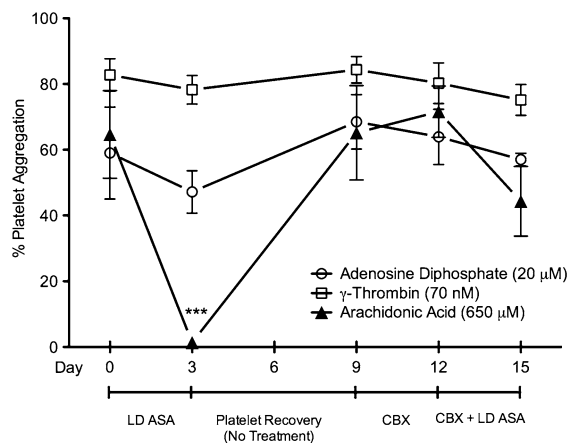


Fig. 6. Treatment of dogs with celecoxib interferes with the effect of low-dose aspirin on ex vivo platelet aggregation. Purpose-bred beagle dogs ($n = 6$, 10–12 kg) were administered low-dose aspirin alone (1.16 mg/kg, p.o.; LD ASA), celecoxib alone (1.43 mg/kg, po bid; CBX), or both celecoxib plus low-dose aspirin (CBX + LD ASA) for a period of three days. At the conclusion of each treatment regimen, platelet-rich plasma was prepared by centrifugation from venous whole blood collected in 3.7% sodium citrate. Ex vivo platelet aggregation responses to three platelet agonists [AA (650 μ M), adenosine diphosphate (20 μ M), and γ -thrombin (70 nM)] were recorded. Data are expressed as the mean \pm SEM. *** indicates $p < 0.001$ when each time point is compared to the same agonist at day 0 by two-way ANOVA.

celecoxib alone, celecoxib plus low-dose aspirin, and low-dose aspirin alone (Fig. 6). Celecoxib was administered at levels equivalent to 100 mg of celecoxib administered to humans twice daily at 8AM and 5PM. Aspirin was administered at 12PM at a dose equivalent to low-dose aspirin administered to humans (81 mg/day). Celecoxib treatment interfered with the ability of low-dose aspirin to block AA-induced platelet aggregation (Fig. 6). The response to aspirin was restored when celecoxib administration was stopped.

Discussion

Our present results establish that COX-2 inhibitors bind tightly to COX-1. In the cases of celecoxib and nimesulide, the binding is rapidly reversible, whereas with DuP697 and NS398 the binding is slowly reversible. The relative potencies of celecoxib in inhibiting AA and adrenic acid oxygenation by ovCOX-1 vs. huCOX-2 suggest that COX-1 has a higher affinity for this coxib than does COX-2. This is important because celecoxib in the form of Celebrex is the most widely prescribed COX-2 inhibitor in the United States. We have also demonstrated that the binding of celecoxib to COX-1 at pharmacologically relevant concentrations interferes with the inactivation of COX-1 by aspirin under conditions in which celecoxib does not block COX-1 activity toward AA. Based on our crystallographic results, we presume that celecoxib binds to the COX active site of one monomer of COX-1 and that, as a consequence, aspirin binding to the partner COX-1 monomer is altered so as to slow the rate of acetylation of the enzyme. In marked contrast, binding of celecoxib to one monomer of COX-1 does not affect the manner in which AA binds and is oxygenated within the COX active site of the partner monomer.

Aspirin is widely used in conjunction with Celebrex to attenuate the cardiovascular side effects of COX-2 inhibitors (6, 15, 16, 19). Studies in humans have suggested that celecoxib does not interfere with the effect of a conventional aspirin tablet containing 324 mg of aspirin (15, 16). However, what is generally considered to be low-dose aspirin (i.e., 81 mg), which is metabolized rapidly to an ineffective concentration, has not been

tested vs. celecoxib. Our in vitro results indicate that celecoxib could interfere with the action of aspirin on COX-1 in vivo, and in our dog model, celecoxib did interfere with the effect of low-dose aspirin. Therefore, it will be important to determine if celecoxib impedes the action of low-dose aspirin in humans. A pharmacological effect of celecoxib on the action of low-dose aspirin on platelet aggregation in humans would necessitate modifying dosing regimens to provide clinically effective COX-2 inhibition while minimizing interference with aspirin inhibition of platelet COX-1.

Methods

Materials. Arachidonic acid and adrenic acid were from Cayman Chemical Co. [$1\text{-}^{14}\text{C}$]-AA (55 mCi/mmol) and [$1\text{-}^{14}\text{C}$ -acetyl]salicylic acid (55 mCi/mmol) were from American Radiolabeled Chemicals. Bicinchoninic acid protein reagent was from Pierce Biochemical.

Expression, Purification, and Assay of ovCOX-1. Protocols for expressing and purifying native ovCOX-1 and huCOX-2 from Sf21 insect cells and assaying COX activities have been reported previously (7, 8, 34, 35). One unit of COX activity is defined as 1 μ mol of O_2 consumed per minute per milligram of enzyme at 37 $^\circ\text{C}$ in the assay mixture. GraphPad Prism version 5.0 was used for graphing K_m and V_{max} .

Quantitation of Aspirin Acetylation. Native ovCOX-1 (5–10 μ M) was incubated with 1-mM [$1\text{-}^{14}\text{C}$ -acetyl]salicylate for different times at 37 $^\circ\text{C}$ essentially as described by Bala et al. (36). Further details are provided in *SI Text*.

Crystallization of Celecoxib/ovCOX-1 Complex. Protein was prepared for crystallization trials as previously described with some modifications (37, 38) that are detailed in *SI Text*. ovCOX-1 (72 μ M dimer) was incubated with 144 μ M heme (Fe^{3+} -protophyrin IX) and 72 μ M celecoxib, and crystallization was performed using the sitting drop vapor diffusion method.

Data Collection and Processing. Diffraction data were collected from crystals in a -135°C nitrogen stream at beam line 21 ID-D, Life Sciences-cat (Argonne National Laboratory, Argonne, IL). Data processing and scaling in space groups $P6_5/22$ and $P6_5$ were performed using HKL2000 (39). Scaling statistics for all data to 2.75 \AA were comparable in both space groups and correct identification of the space group could not easily be definitively established. The R_{merge} for all data in space groups $P6_5/22$ and $P6_5$ was 6.2% (57.7% in outer shell) and 6.3% (54.1% in outer shell), respectively. Analysis of the intensity statistics using phenix.xtriage suggested that crystal twinning could not be ruled out in space group $P6_5$ with an estimated twin fraction equal to 0.478 (Table S1). Statistics for the data collection, processing, and crystallographic refinement of the final refined model are shown in Table S2.

Molecular Replacement and Crystallographic Refinement. The starting coordinates were taken from the α -methyl-4-biphenylacetic acid/ovCOX-1 structure (1Q4G). Structure solution by molecular replacement was performed with PHASER (40) in space groups $P6_5/22$ and $P6_5$ using the coordinates of the protein atoms alone. Initial model building and refinement in both space groups had varying improvements on the electron density but the R_{free} in either space did not progress below 29–31% despite nearly completing the model building. However, when using a single round of simulated annealing and rigid body refinement with the twin operator h, -h, -k, -l in PHENIX version 1.3 (41), the R_{factor} and R_{free} improved by about 5%. Further model building progressively improved refinement statistics. The dictionary files used to build the model were generated using PRODRG2 (42) from the appropriate Protein Data Bank (PDB) coordinates obtained from either the HIC-up or ChemDB servers. Celecoxib, N-linked carbohydrates, and detergents were built into the electron density using COOT (43). The resulting model was subjected to iterative cycles of model building, inspection, and individual ADP refinement with tensor/libation/screw and noncrystallographic symmetry restraints. The refinement converged with an R_{factor} of 21.98% for all data to 2.75 \AA , with an R_{free} value of 24.44%. Structure validation was performed using PROCHECK (44) and Molprobit (45). Ligand contact distances were determined using both the ligand-protein contacts and contacts of structural units (46) and PDBSum servers (47). Figures were generated using MacPyMOL (48). Multiple occupancy refinement trials were performed using different starting occupancy values. We estimated occupancy in monomer A to be nearly complete, while monomer B was less than 50% based on the B factors of the inhibitor relative to the B factors of neighboring amino acids.

Effect of Celecoxib and Aspirin on Ex Vivo Platelet Aggregation. Purpose-bred beagle dogs (six, 10–12 kg) were administered aspirin (ASA) alone (1.16 mg/kg, *per os* (p.o.)), celecoxib alone (1.43 mg/kg, p.o. twice a day), or the combination of both ASA and celecoxib for a period of days. At the conclusion of each treatment regimen, whole blood was collected and ex vivo platelet aggregation responses to platelet agonists (AA and adenosine diphosphate) were recorded.

1. van der Donk W, Tsai A, Kulmacz R (2002) The cyclooxygenase reaction mechanism. *Biochemistry*, 41(52):15451–15458.
2. Rouzer C, Marnett L (2003) Mechanism of free radical oxygenation of polyunsaturated fatty acids by cyclooxygenases. *Chem Rev*, 103(6):2239–2304.
3. Smith WL (2008) Nutritionally essential fatty acids and biologically indispensable cyclooxygenases. *Trends Biochem Sci*, 33(1):27–37.
4. Schneider C, Pratt DA, Porter NA, Brash AR (2007) Control of oxygenation in lipoxygenase and cyclooxygenase catalysis. *Chem Biol*, 14(5):473–488.
5. Rouzer CA, Marnett LJ (2008) Non-redundant Functions of Cyclooxygenases: Oxygenation of Endocannabinoids. *J Biol Chem*, 283(13):8065–8069.
6. Grosser T, Fries S, FitzGerald GA (2006) Biological basis for the cardiovascular consequences of COX-2 inhibition: Therapeutic challenges and opportunities. *J Clin Invest*, 116(1):4–15.
7. Yuan C, Rieke CJ, Rimon G, Wingerd BA, Smith WL (2006) Partnering between monomers of cyclooxygenase-2 homodimers. *Proc Natl Acad Sci USA*, 103(16):6142–6147.
8. Yuan C, et al. (2009) Cyclooxygenase allosterism, fatty acid-mediated cross-talk between monomers of cyclooxygenase homodimers. *J Biol Chem*, 284(15):10046–10055.
9. Kulmacz RJ, Lands WEM (1985) Stoichiometry and kinetics of the interaction of prostaglandin H synthase with anti-inflammatory agents. *J Biol Chem*, 260(23):12572–12578.
10. Prusakiewicz J, Duggan K, Rouzer C, Marnett L (2009) Differential sensitivity and mechanism of inhibition of COX-2 oxygenation of arachidonic acid and 2-arachidonoylglycerol by ibuprofen and mefenamic acid. *Biochemistry*, 49:7353–7355.
11. Rosenstock M, Danon A, Rimon G (1999) PGHS-2 inhibitors, NS-398 and DuP-697, attenuate the inhibition of PGHS-1 by aspirin and indomethacin without altering its activity. *Biochim Biophys Acta*, 1440(1):127–137.
12. Rosenstock M, Danon A, Rubin M, Rimon G (2001) Prostaglandin H synthase-2 inhibitors interfere with prostaglandin H synthase-1 inhibition by nonsteroidal anti-inflammatory drugs. *Eur J Pharmacol*, 412(1):101–108.
13. Burde T, Rimon G (2002) On the interaction of specific prostaglandin H synthase-2 inhibitors with prostaglandin H synthase-1. *Eur J Pharmacol*, 453:167–173.
14. Ouellet M, Riendeau D, Percival MD (2001) A high level of cyclooxygenase-2 inhibitor selectivity is associated with a reduced interference of platelet cyclooxygenase-1 inactivation by aspirin. *Proc Natl Acad Sci USA*, 98(25):14583–14588.
15. K Wilner, et al. (2002) Celecoxib does not affect the antiplatelet activity of aspirin in healthy volunteers. *J Clin Pharmacol*, 42(9):1027–1030.
16. Gladding P, et al. (2008) The antiplatelet effect of six non-steroidal anti-inflammatory drugs and their pharmacodynamic interaction with aspirin in healthy volunteers. *Am J Cardiol*, 101(7):1060–1063.
17. Greenberg HE, et al. (2000) A new cyclooxygenase-2 inhibitor, rofecoxib (VIOXX), did not alter the antiplatelet effects of low-dose aspirin in healthy volunteers. *J Clin Pharmacol*, 40(12):1509–1515.
18. Catella-Lawson F, et al. (2001) Cyclooxygenase inhibitors and the antiplatelet effects of aspirin. *N Engl J Med*, 345(25):1809–1817.
19. Solomon SD, et al. (2008) Cardiovascular risk of celecoxib in 6 randomized placebo-controlled trials: The cross trial safety analysis. *Circulation*, 117(16):2104–2113.
20. Hennen JK, et al. (2001) Effects of selective cyclooxygenase-2 inhibition on vascular responses and thrombosis in canine coronary arteries. *Circulation*, 104(7):820–825.
21. Copeland RA, et al. (1994) Mechanism of selective inhibition of the inducible isoform of prostaglandin G/H synthase. *Proc Natl Acad Sci USA*, 91(23):11202–11206.
22. Laneville O, et al. (1994) Differential inhibition of human prostaglandin endoperoxide H synthases-1 and -2 by nonsteroidal anti-inflammatory drugs. *J Pharmacol Exp Ther*, 271(2):927–934.
23. Rieke CJ, Mulichak AM, Garavito RM, Smith WL (1999) The role of arginine 120 of human prostaglandin endoperoxide H synthase-2 in the interaction with fatty acid substrates and inhibitors. *J Biol Chem*, 274(24):17109–17114.
24. Walker M, et al. (2001) A three-step kinetic mechanism for selective inhibition of cyclo-oxygenase-2 by diarylheterocyclic inhibitors. *Biochem J*, 357(Pt 3):709–718.

ACKNOWLEDGMENTS. We thank Dr. Michael J. Malkowski (Hauptman-Woodward Institute and Department of Structural Biology, State University of New York, Buffalo) for a careful reading of the manuscript. These studies were supported in part by US Public Health Service grants from the National Institutes of Health—National Institute of General Medical Sciences (W.L.S. and R.C.T.) and a postdoctoral fellowship from the Heart and Stroke Foundation of Canada (R.S.S.).

25. Liu W, Cao D, Oh SF, Serhan CN, Kulmacz RJ (2006) Divergent cyclooxygenase responses to fatty acid structure and peroxide level in fish and mammalian prostaglandin H synthases. *FASEB J*, 20(8):1097–1108.
26. Skarke C, et al. (2006) The cyclooxygenase 2 genetic variant –765G>C does not modulate the effects of celecoxib on prostaglandin E2 production. *Clin Pharmacol Ther*, 80(6):621–632.
27. Bae SK, et al. (2008) Determination of acetylsalicylic acid and its major metabolite, salicylic acid, in human plasma using liquid chromatography-tandem mass spectrometry: Application to pharmacokinetic study of Astrix in Korean healthy volunteers. *Biomed Chromatogr*, 22(6):590–595.
28. Gengo FM, et al. (2008) Prevalence of platelet nonresponsiveness to aspirin in patients treated for secondary stroke prophylaxis and in patients with recurrent ischemic events. *J Clin Pharmacol*, 48(3):335–343.
29. DeWitt DL (1999) Cox-2-selective inhibitors: The new super aspirins. *Mol Pharmacol*, 55(4):625–631.
30. Suleyman H, Cadirci E (2008) Nimesulide is a selective COX-2 inhibitory, atypical non-steroidal anti-inflammatory drug. *Curr Med Chem*, 15:278–283.
31. Luong C, et al. (1996) Flexibility of the NSAID binding site in the structure of human cyclooxygenase-2. *Nat Struct Biol*, 3:927–933.
32. Kurumbail RG, et al. (1996) Structural basis for selective inhibition of cyclooxygenase-2 by anti-inflammatory agents. *Nature*, 384(6610):644–648.
33. Malkowski MG, Ginell S, Smith WL, Garavito RM (2000) The x-ray crystal structure of prostaglandin endoperoxide H synthase-1 complexed with arachidonic acid. *Science*, 289:1933–1937.
34. Liu J, et al. (2007) Prostaglandin endoperoxide H synthases: Peroxidase hydroperoxide specificity and cyclooxygenase activation. *J Biol Chem*, 282:18233–18244.
35. Wada M, et al. (2007) Specificities of enzymes and receptors of prostaglandin pathways with arachidonic acid and eicosapentaenoic acid derived substrates and products. *J Biol Chem*, 282:22254–22266.
36. Bala M, et al. (2008) Acetylation of prostaglandin H2 synthases by aspirin is inhibited by redox cycling of the peroxidase. *Biochem Pharmacol*, 75(7):1472–1481.
37. Harman CA, Rieke CJ, Garavito RM, Smith WL (2004) Crystal structure of arachidonic acid bound to a mutant of prostaglandin endoperoxide H synthase-1 that forms predominantly 11-hydroperoxyeicosatetraenoic acid. *J Biol Chem*, 279(41):42929–42935.
38. Harman CA, et al. (2007) Structural basis of enantioselective inhibition of cyclooxygenase-1 by 5- α -substituted indomethacin ethanalamides. *J Biol Chem*, 282(38):28096–28105.
39. Otwinowski Z, Minor W (1997) Processing of x-ray diffraction data collected in oscillation mode. *Method Enzymol*, 276:307–326.
40. McCoy AJ, Grosse-Kunstleve RW, Storoni LC, Read RJ (2005) Likelihood-enhanced fast translation functions. *Acta Crystallogr D*, 61(Pt 4):458–464.
41. Adams PD, et al. (2002) PHENIX: Building new software for automated crystallographic structure determination. *Acta Crystallogr D*, 58(Pt 11):1948–1954.
42. Schuttelkopf AW, van Aalten DM (2004) PRODRG: A tool for high-throughput crystallography of protein-ligand complexes. *Acta Crystallogr D*, 60(Pt 8):1355–1363.
43. Emsley P, Cowtan K (2004) Coot: Model-building tools for molecular graphics. *Acta Crystallogr D Biol Crystallogr*, 60(Pt 12, Pt 1):2126–2132.
44. Laskowski RA, MacArthur MW, Moss DS, Thornton JM (1993) PROCHECK: A program to check the stereochemical quality of protein structures. *J Appl Cryst*, 26:283–291.
45. Davis IW, et al. (2007) MolProbity: all-atom contacts and structure validation for proteins and nucleic acids. *Nucleic Acids Res*, 35(Suppl 2):W375–383.
46. Sobolev V, Sorokine A, Prilusky J, Abola E, Edelman M (1999) Automated analysis of interatomic contacts in proteins. *Bioinformatics*, 15(4):327–332.
47. Laskowski R, et al. (1997) PDBsum: A web-based database of summaries and analyses of all PDB structures. *Trends Biochem Sci*, 22(12):488–490.
48. DeLano WL (2008) *The PyMOL Molecular Graphics System* (DeLano Scientific, Palo Alto, CA).